Zeptosecond dynamics of superheavy element synthesis reactions: the role of sequential fission

S.L. Hayles[1,*], J. Buete[1], K.J. Cook[1], D.J. Hinde[1], M. Dasgupta[1], L.T. Bezzina[1,**], H. Haba[2], M.K. Lakelin[1], H. Lee[1], C.C. Seabra[1], T. Tran[1], and M.M. Webber[1]

[1]Department of Nuclear Physics and Accelerator Applications, Research School of Physics, The Australian National University, Canberra, ACT 2601, Australia.
[2]Nishina Center for Accelerator-Based Science, RIKEN, Wako, Saitama 351-0198, Japan

Abstract. Our understanding of quasifission and thus superheavy element formation may be hindered by sequential fission, a secondary process that results in three final quasifission fragments rather than the expected two. This net three-body process is typically rejected or not detected in typical binary measurements, potentially eliminating the fastest outcomes of superheavy element synthesis reactions and leading to an incomplete understanding of the true primary reaction dynamics. To overcome this, the CUBE detector array at ANU was used to measure two- and three-body outcomes of reactions of ^{28}Si + ^{248}Cm, allowing us to uncover the full mass split distribution in the primary binary decay. For fragments with a mass greater than ^{208}Pb, we find that including three-body outcomes enhances the cross-section by up to two orders of magnitude over the two-body quasifission cross-sections alone. These results present clear evidence that sequential fission plays a significant role in superheavy element synthesis reactions and should be accounted for in future studies.

1 Introduction

Superheavy elements provide a valuable opportunity to expand our understanding of fundamental quantum and nuclear physics. The production of such elements is severely hindered by faster competing processes such as quasifission and fusion-fission [1], illustrated in Figure 1. Once capture occurs, the dominant outcome is quasifission, where the dinucleus separates prior to full equilibration, preventing the formation of a compact compound nucleus [1]. The probability of quasifission, P_{QF}, is complementary to the probability of successfully forming a compound nucleus, $P_{\mathrm{CN}} = 1 - P_{\mathrm{QF}}$ [2].

P_{QF} is strongly dependent on the reaction entrance channel [3], meaning that an optimal choice of reaction can drastically increase P_{CN}. This is why all known elements heavier than Nh (Z = 113) were initially formed with the doubly magic ^{48}Ca: using this nucleus as a projectile acts to minimise P_{QF}, hence maximising P_{CN} compared to reaction pathways using beams of heavier elements [4].

The lack of material to make long-lived targets heavier than Cf (Z = 98) means that we cannot use ^{48}Ca to produce elements past 118 [5]. To proceed, we must rely on reactions with heavier beams such as Ti or Cr [4, 6]. While we know that these reactions have a lower chance of forming a superheavy element [4, 6], we currently do not have a strong enough constraint on P_{CN} to accurately predict superheavy element formation cross-sections. In general, P_{CN} is poorly understood [7], largely due to the complicated nature of non-equilibrium outcomes such as quasifission. To improve our chance of creating a new element, we therefore need to improve our understanding of the fundamental dynamics of quasifission.

Experimentally, we investigate quasifission by measuring observables such as the mass, angle and total kinetic energy of the fragments. However, recent work [8] has revealed that typical quasifission measurements may be incomplete due to the presence of *sequential fission*, where the heavy fragment of a primary quasifission reaction further decays in a fission-like process [8–10].

Sequential fission is a possible decay pathway for any nucleus produced in a fast primary reaction with excitation energy above its fission barrier [8–10]. This becomes increasingly likely in superheavy element synthesis reactions, where a large proportion of multi-nucleon transfer, deep-inelastic collisions, and fast quasifission outcomes (all of which occur on a 10^{-21} s timescale) form fragments heavier than ^{208}Pb [8], whose fission barriers decrease with increasing atomic number [11]. As a result, the effect of sequential fission is largest for the fastest outcomes that follow minimal mass transfer and occur within just a few zeptoseconds. Indirect measurements of the three-body cross-section in reactions of ^{50}Ti with a variety of actinides targets support this: without accounting for sequential fission, many of these fast outcomes are missing and capture cross-sections are suppressed compared to calculations [8].

*e-mail: Sophie.Hayles@anu.edu.au
**Present address: Laboratory of Ion Beam Physics, ETH Zürich, HPK G 31, Otto-Stern-Weg 5, 8093 Zürich, Switzerland.

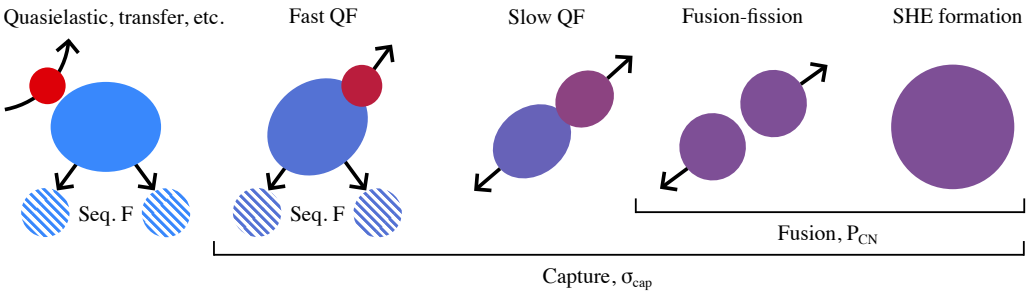

Figure 1. Potential outcomes of superheavy element synthesis reactions, ordered by increasing reaction timescale (see text). Capture and fusion outcomes are indicated, with probabilities given by the capture cross-section, σ_{cap}, and probability of compound nucleus formation, P_{CN}, respectively. Sequential fission follows the fastest primary reactions, resulting in three final reaction products.

Sequential fission results in a net three-body outcome. Typical binary measurements assume that all momentum from the reactants is transferred to two heavy fragments. This is not the case if we measure two fragments of an overall three-body outcome, leading to a rejection of these events. As a result, many current measurements of quasi-fission that involve actinide targets are incomplete, missing the fast primary outcomes that resulted in sequential fission [8]. To understand the dynamics driving the primary two-body reaction that occurs prior to sequential fission, we therefore need to include both two-body *and* three-body sequential fission outcomes.

2 Methodology

The experiment was performed at the Heavy Ion Accelerator Facility at ANU, using the 14UD tandem accelerator to produce beams of ^{28}Si at centre-of-mass energies E_{cm} ranging from 0.9 to 1.0 of the capture barrier [12], V_{B} = 144.2 MeV. These beams impinged onto a target of ^{248}Cm$(NO_3)_3$ that had an energy loss equivalent to 55.696 μg/cm^2 of elemental ^{248}Cm, supported on a 198 μg/cm^2 aluminium backing located downstream of the target. Event-by-event corrections were made to account for energy lost through the target and backing materials [13].

The two- and three-body outcomes of ^{28}Si + ^{248}Cm reactions forming the superheavy ^{276}Ds (Z = 110) were measured in coincidence using the CUBE detector array [3, 7, 14, 15]. This array comprises three large-area multiwire proportional counters (MWPCs) to measure each fragment's position and time-of-flight, configured as shown in Ref. [16]. Two-body events were selected by requiring full momentum transfer from the reactants to the two resulting fragments, removing contamination from reactions with other target materials or incomplete three-body events. The fragment velocities, v_i, and the mass-ratio at scission, M_{R}, were reconstructed using the kinematic coincidence method [14]. Using this method, CUBE's mass and angular resolution are 1.8 amu and 0.3° respectively [17]. Uncertainty in the energy loss of fragments through the target and backing is the largest source of this overall experimental uncertainty [17].

Fragment mass numbers were extracted by multiplying M_{R} by the total mass of the projectile-target system, A_{CN}. If neutron emission prior to scission occurs, decreasing A_{CN}, the extracted fragment mass A_{F} will also shift. For fusion-fission outcomes, where we expect evaporation to be most likely, we performed GEF calculations [18] to predict the mean pre-scission neutron multiplicity. At the highest energy, $E_{\mathrm{cm}}/V_{\mathrm{B}}$ = 1.00, we found that on average only one neutron is evaporated prior to scission. This would correspond to a shift in the symmetric fragment masses by 0.5 amu. As we move towards outcomes involving less mass-equilibration, such as fast quasifission, the excitation energy and thus pre-scission neutron multiplicity is expected to decrease compared to fusion-fission [19]. We therefore expect that the extracted fragment masses for these outcomes will be largely unperturbed by neutron evaporation from the dinucleus.

2.1 CUBE triple coincidence mass reconstruction

Three-body events were identified by requiring that a fragment was detected in coincidence on each of CUBE's three MWPCs. The method to reconstruct the masses of three coincident fragments assumes full momentum transfer to three products, requiring that their momenta sum to zero in the centre-of-mass frame. The mass ratio between any two fragments can therefore be determined by

$$\frac{m_i}{m_j} = \frac{|v_j| \sin \alpha_{jk}}{|v_i| \sin \alpha_{ik}}, \tag{1}$$

where v_i is the velocity of fragment i in the centre of mass frame, and α_{ij} is the angle between fragments i and j, as indicated in the inset of Figure 2.

Momentum conservation enforces that all three fragments produced from a common beam-target interaction lie in one plane in the centre-of-mass frame. We will refer to this plane as the sequential fission fragment plane. If this is the case, the sum of the angles between fragments $\alpha_{\mathrm{sum}} = \alpha_{12} + \alpha_{23} + \alpha_{31}$ must be 360°. The total angle sum, α_{sum}, is largely unaffected by perturbations to the fragments' velocity vectors such as those caused by angular straggling in the target, neutron evaporation, or detector resolution. A change in velocity that occurs along the sequential fission fragment plane will not affect α_{sum}: any change in angle α_{ij} will be compensated by a complementary change in another angle, leaving α_{sum} unchanged. In contrast, a perturbation of one fragment perpendicular to the sequential fission fragment plane *will* change α_{sum}. If fragment i is perturbed out of plane by an angle ϕ, the

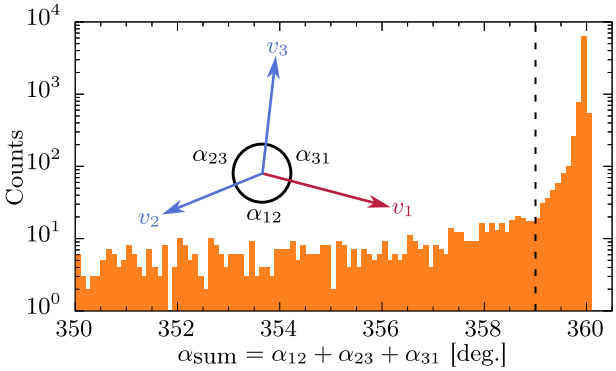

Figure 2. The sum of the measured angles between three fragments for the reaction ^{28}Si + ^{248}Cm at $E_{\rm cm}/V_{\rm B}$ = 0.93. Events with an angle sum less than the dashed line at 359° did not lie on a plane and therefore did not conserve momentum. The inset shows the velocities and angles required to reconstruct the masses of three-body events.

new angle α'_{ij} will change relative to the unperturbed α_{ij} according to

$$\frac{\cos\alpha'_{ij} - \cos\alpha_{ij}}{\cos\alpha_{ij}} \sim \tan^2\phi. \tag{2}$$

From this, it follows that $\alpha_{\rm sum}$ is relatively insensitive to small perturbations. For example, if two fragments are initially separated by α_{ij} = 120° and one is perturbed by ϕ = 1° out of the sequential fission plane, α_{ij} will only change by 0.005° and hence $\alpha_{\rm sum}$ by 0.010°. This means that requiring $\alpha_{\rm sum}$ > 359° is sufficient to remove events that do not conserve momentum while accounting for expected variation in the fragment angles due to the aforementioned experimental or measurement effects. Figure 2 shows the distribution of $\alpha_{\rm sum}$ measured for the reaction ^{28}Si + ^{248}Cm at $E_{\rm cm}/V_{\rm B}$ = 0.93. This distribution is strongly peaked near 360°, with about 85% of three-body outcomes having an $\alpha_{\rm sum}$ > 359°. The 15% of events outside of this range involved triple coincidences that did not originate from a common beam-target interaction and therefore did not conserve momentum.

It is unlikely that the heavy fragment that undergoes sequential fission is carrying sufficient excitation energy to evaporate more than a single neutron and still fission. To conserve mass, we therefore require $A_{\rm CN} = m_1 + m_2 + m_3$. This allows us to write the mass of fragment i as

$$m_i = A_{\rm CN}\left(\frac{m_j}{m_i} + \frac{m_k}{m_i} + 1\right)^{-1} \tag{3}$$

using the mass ratios defined in Equation 1. Using this method allows us to reconstruct three-body outcomes with CUBE for the first time.

2.2 Triple coincidence cross-section determination

The significance of sequential fission in ^{28}Si + ^{248}Cm was determined by investigating the impact these events had on the differential cross-section of fast outcomes such as deep-inelastic collisions, multinucleon transfer and quasifission. In the binary case, we normalise to Rutherford scattering measured by silicon monitors at forward angles. This allows us to account for CUBE's solid angle and efficiency for measuring two-body events, which is ~25%.

In the ternary case, we have to apply a further correction to account for the decrease in efficiency that arises when we require coincident measurements of three fragments. This efficiency correction term is calculated using a Monte Carlo simulation to determine the proportion of three-body events that can be detected by CUBE. To start this iterative process, we input the measured distributions of the light fragment's mass, angle and kinetic energy, and the mass split and total kinetic energy of the sequentially fissioning system. Due to the large angular coverage of CUBE, these measured distributions are continuous in our range of interest, where the light fragment angle is greater than 50°. The simulation ends after 1 million of the generated events involve three fragments detected with the current CUBE configuration.

This process provides the detector efficiency matrix as a function of the light fragment's mass and angle. For a given light fragment, this matrix tells us how likely it is that all three fragments were successfully measured by CUBE. After producing the first efficiency matrix, we use it to create an efficiency-corrected input distribution. This input distribution is used in the next iteration of the simulation, generating an updated efficiency matrix. We repeat this process until the efficiency matrices and overall detection efficiencies converge. For reactions in this work, the overall efficiency for three-body events converged to ~5%. The primary factor limiting this three-body efficiency is the incomplete geometric ϕ coverage of the CUBE detectors, which is known. The final efficiency matrix is used in conjunction with the solid-angle normalisation to convert our measured three-body yields to cross-sections.

3 Results and Discussion

3.1 Three-body fragment mass distribution

The mass distribution of three fragments arising from the reaction of ^{28}Si + ^{248}Cm at $E_{\rm cm}/V_{\rm B}$ = 0.93 is shown in Figure 3. The reconstructed masses show one light fragment from the primary binary reaction highlighted in red. The mass of this fragment is peaked at the ^{28}Si projectile mass, indicated by the dashed line at $A_{\rm F}$ = 28. There is also a tail extending to fragments of heavier mass, indicating that a small proportion of measured three-body events occurred after the transfer of up to 40 nucleons from the target to the projectile. Persisting at all energies, this result indicates that a majority of sequential fission events result from quasielastic processes, and a small fraction from multi-nucleon transfer and fast quasifission.

The complementary particles appear as sequential fission-like fragments, forming the doubly-peaked hatched mass distribution in Figure 3. Combining results for all energies, the peaks of this distribution were located at $A_{\rm F}$ = 106.2 ± 0.4 and 138.8 ± 0.5. The peak positions of our sequential fission fragment masses are in excellent agreement with the measured peak masses of ^{248}Cm spontaneous fission fragments [17, 20–22], an example of which is shown by the grey lines in Figure 3. There is

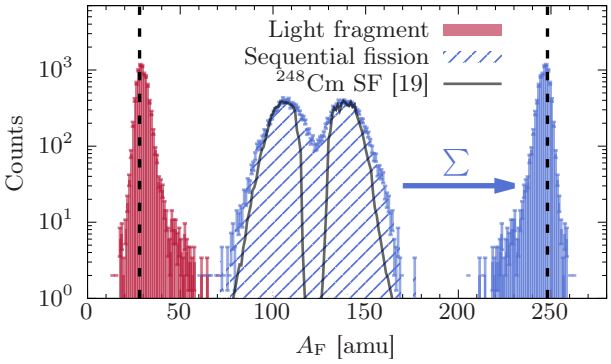

Figure 3. Mass distribution of three-body outcomes of the reaction ^{28}Si + ^{248}Cm at $E_{cm}/V_B = 0.93$. The measured light fragment of the primary reaction is shown in red, and mass distribution of the two sequential fission fragment in blue (hatched). Summing the masses of the two sequential fission fragments produces the distribution for the primary target-like fragment shown in blue (filled). The grey lines shows a mass distribution for the spontaneous fission (SF) of ^{248}Cm [20].

some increased spread in our distribution due to the difference in excitation energy between the low-energy spontaneous fission measurements and the excited nucleus that undergoes sequential fission. In addition, contributions from the fission of actinide nuclei other than ^{248}Cm result in a natural widening of our overall distribution. Despite this, the agreement of the peak positions of our measured distribution with the ^{248}Cm sequential fission distribution allows us to attribute these events to the sequential fission of a nucleus near ^{248}Cm following minimal evaporation.

The masses of the two sequential fission fragments were summed to recover the mass of the heavy fragment produced in the primary binary outcome, shown in solid blue. Complementary to the light fragment, the heavy fragment's mass is peaked at $A_F = 248$ and extends down to $A_F = 208$. These primary outcomes occur in the first moments of capture and span the gap between quasifission and scattering events.

3.2 Incorporating two- and three-body outcomes

We can now investigate the full primary mass-split by combining the three-fragment results from Figure 3 with two-body outcomes also measured by CUBE. Figure 4(a) shows a section of the mass-angle distribution (MAD) for two-body outcomes alone. In this MAD, we have focussed on the mass-angle region where we expect to measure the highest proportion of heavy fragments resulting from fast outcomes, where sequential fission is expected to be most influential. This is also the angular region in which our three-body detection efficiency is highest (up to 9%), and independent of the mass of the light fragment. Indicated by the arrow in Figure 4(a), there is clear separation of quasielastic events, centred at $A_F = 248$, and fast quasifission events.

At all measured energies of the ^{28}Si + ^{248}Cm reaction, fast quasifission fragment masses were peaked at $A_F = 83 \pm 3$ and 193 ± 3, in agreement with previous work studying ^{28}Si, ^{36}S + ^{238}U [7, 23]. The observed peaks in yield below $A_F = 208$ make it difficult to reconcile these outcomes with ^{208}Pb shell effects. In contrast, outcomes of higher Z_1Z_2 reactions involving ^{48}Ca or ^{50}Ti projectiles on actinide targets [8] *are* peaked near ^{208}Pb, which is typically attributed to ^{208}Pb shell effects [24] or sequential fission [8]. It is clear that the quasifission outcomes in reactions with actinide nuclides rapidly change as the projectile mass changes. We attribute this difference to an increased sticking time for the lighter projectiles, allowing mass flow past ^{208}Pb.

Incorporating previously missing three-body outcomes allows us to probe the complete primary binary outcome. This is shown in Figure 4(b) for ^{28}Si + ^{248}Cm at $E_{cm}/V_B = 0.93$. In comparison to Figure 4(a), we can see that accounting for sequential fission begins to fill the gap between quasielastic and fast quasifission regions.

To quantify the impact of including three-body outcomes, we project over the angular range in Figures 4(a) and (b) to produce the differential cross-section as a function of fragment mass. The resulting mass distribution in Figure 4(c) shows the cross-section for pure two-body primary outcomes (orange), and all primary outcomes, obtained by including sequential fission (blue). Including three-body sequential fission events results in an enhancement of the differential cross-section for fragments heavier

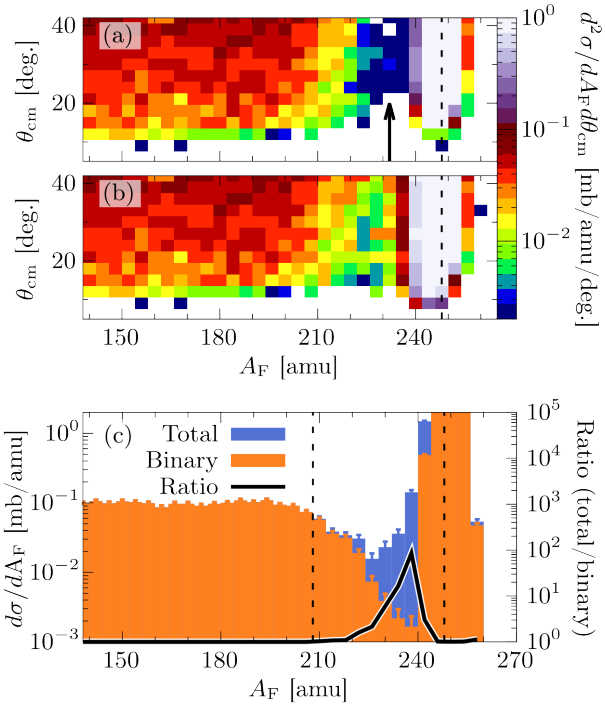

Figure 4. Results of the reaction ^{28}Si + ^{248}Cm at $E_{cm}/V_B = 0.93$. (a) A MAD for two-body events over the angular range 5° to 42°. The dashed line indicates the mass of ^{248}Cm and the arrow indicates the region between quasielastic and fast quasifission events with low yield due to sequential fission. (b) The MAD for all primary reactions, obtained by summing the binary MAD and previously unaccounted for three-body sequential fission outcomes. (c) Mass distributions for two-body outcomes and all primary outcomes, obtained by summing over angles shown in (a) and (b) respectively (scale on left axis). The ratio of the total to binary distributions is shown in black (scale on right axis). Dashed lines indicate the masses of ^{208}Pb and ^{248}Cm.

than ^{208}Pb and lighter than ^{248}Cm. In particular, the cross-section for fragments a few nucleons lighter than ^{248}Cm is enhanced by up to two orders of magnitude. This is shown by the ratio of the total differential cross-section to the two-body cross-section alone (black line), whose scale is on the right axis of Figure 4(c). Primary mass distributions that are produced as a function of the angles in 4(b) reveal no significant variation in the role of sequential fission between 5° and 42°.

4 Conclusions

These results show that sequential fission can form a significant fraction of the binary yield of fragments heavier than ^{208}Pb and lighter than the target, even for a light projectile like ^{28}Si. We expect the effect of sequential fission to be even more significant in higher Z_1Z_2 systems, where the sticking time is likely shorter, giving less potential for mass equilibration past ^{208}Pb [8].

Crucially, accounting for sequential fission means that the distinction between quasielastic and fast quasifission outcomes is far less clear than previous work seems to imply. It is likely that the distinction between these types of outcomes will be entirely blurred in higher Z_1Z_2 systems, as indicated in Ref. [8]. This would result in a smooth, monotonic evolution from quasielastic to fast quasifission outcomes, similar to lower Z_1Z_2 systems [25]. As well as changing our understanding of quasifission and mass equilibration, this result also has significant implications for how we define and distinguish capture from outcomes such as deep-inelastic collisions or multinucleon transfer. Measuring three-body events caused by sequential fission is therefore a necessity when studying the first few zeptoseconds of superheavy element synthesis reactions.

Acknowledgements

The authors acknowledge support from the Australian Research Council through Discovery Grants DE230100197, DP230101028, DP200100601 and DP250101791. Support for the Heavy Ion Accelerator Facility operations from the Australian National Collaborative Research Infrastructure (NCRIS) HIA project is acknowledged. S.L.H., H.L., T.T. and M.M.W. acknowledge support from an Australian Government Research Training Program (RTP) Scholarship.

References

[1] D.J. Hinde et al., Experimental studies of the competition between fusion and quasifission in the formation of heavy and superheavy nuclei, Progress in Particle and Nuclear Physics **118**, 103856 (2021). 10.1016/j.ppnp.2021.103856

[2] C.E. Düllmann, How elements up to 118 were reached and how to go beyond, EPJ Web of Conferences **163**, 00015 (2017). 10.1051/epjconf/201716300015

[3] R.G. Thomas et al., Entrance channel dependence of quasifission in reactions forming ^{220}Th, Phys. Rev. C **77**, 034610 (2008). 10.1103/PhysRevC.77.034610

[4] Y.T. Oganessian et al., Investigation of reactions with ^{50}Ti and ^{54}Cr for the synthesis of new elements, Phys. Rev. C **112**, 014603 (2025). 10.1103/k2g4-5k7x

[5] J.B. Roberto et al., Actinide targets for the synthesis of super-heavy elements, Nuclear Physics A **944**, 99 (2015). 10.1016/j.nuclphysa.2015.06.009

[6] J.M. Gates et al., Toward the discovery of new elements: Production of livermorium (z = 116) with ^{50}Ti, Phys. Rev. Lett. **133**, 172502 (2024). 10.1103/PhysRevLett.133.172502

[7] R. du Rietz et al., Mapping quasifission characteristics and timescales in heavy element formation reactions, Phys. Rev. C **88**, 054618 (2013). 10.1103/PhysRevC.88.054618

[8] D.Y. Jeung et al., Sequential fission and the influence of ^{208}Pb closed shells on the dynamics of superheavy element synthesis reactions, Phys. Lett. B **837**, 137641 (2023). 10.1016/j.physletb.2022.137641

[9] G. Guarino et al., Mass drift in reactions between a heavy and a light nucleus, Nuclear Physics A **424**, 157 (1984). 10.1016/0375-9474(84)90133-7

[10] J.V. Kratz et al., Mass-yield distributions in the reaction of ^{84}Kr ions with ^{238}U, Phys. Rev. Lett. **33**, 502 (1974). 10.1103/PhysRevLett.33.502

[11] P. Möller et al., Fission barriers at the end of the chart of the nuclides, Phys. Rev. C **91**, 024310 (2015). 10.1103/PhysRevC.91.024310

[12] D.Y. Jeung et al., Energy dissipation and suppression of capture cross sections in heavy ion reactions, Phys. Rev. C **103**, 034603 (2021). 10.1103/PhysRevC.103.034603

[13] J.F. Ziegler et al., SRIM – The stopping and range of ions in matter (2010), Nuclear Instruments and Methods in Physics Research Section B: Beam Interactions with Materials and Atoms **268**, 1818 (2010). 10.1016/j.nimb.2010.02.091

[14] D.J. Hinde et al., Conclusive evidence for the influence of nuclear orientation on quasifission, Phys. Rev. C **53**, 1290 (1996). 10.1103/PhysRevC.53.1290

[15] H.M. Albers et al., Zeptosecond contact times for element Z=120 synthesis, Phys. Lett. B **808**, 135626 (2020). 10.1016/j.physletb.2020.135626

[16] T. Banerjee et al., Systematic evidence for quasifission in ^{9}Be-,^{12}C- and ^{16}O-induced reactions forming ^{258,260}No, Phys. Rev. C **102**, 024603 (2020). 10.1103/PhysRevC.102.024603

[17] A. Berriman et al., Energy dependence of p + ^{232}Th fission mass distributions: Mass-asymmetric standard I and standard II modes, and multi-chance fission, Phys. Rev. C **105**, 064614 (2022). 10.1103/PhysRevC.105.064614

[18] K.H. Schmidt et al., General Description of Fission Observables: GEF Model Code, Nuclear Data Sheets **131**, 107 (2016). 10.1016/j.nds.2015.12.009

[19] D.J. Hinde et al., Neutron emission as a probe of fusion-fission and quasifission dynamics, Phys. Rev. C **45**, 1229 (1992). 10.1103/PhysRevC.45.1229

[20] T.R. England, B.F. Rider, Evaluation and compilation of fission product yields 1993 (1995). 10.2172/10103145

[21] K.F. Flynn et al., Mass distributions for the spontaneous fission of ^{248}Cm and ^{250}Cf, Journal of Inorganic and Nuclear Chemistry **39**, 759 (1977). 10.1016/0022-1902(77)80149-8

[22] R. Brandt et al., Mass and energy distributions in the spontaneous fission of some heavy isotopes, Phys. Rev. **131**, 2617 (1963). 10.1103/PhysRev.131.2617

[23] K. Nishio et al., Evidence for quasifission in the subbarrier reaction of ^{30}Si + ^{238}U, Phys. Rev. C **82**, 044604 (2010). 10.1103/PhysRevC.82.044604

[24] C. Simenel et al., Comparison of fission and quasifission modes, Phys. Lett. B **822**, 136648 (2021). 10.1016/j.physletb.2021.136648

[25] K. Banerjee et al., Mechanisms suppressing superheavy element yields in cold fusion reactions, Phys. Rev. Lett. **122**, 232503 (2019). 10.1103/PhysRevLett.122.232503